

## AN ENERGY SOURCE FOR MODELING HCDA BUBBLES\*

D. W. PLOEGER, D. J. CAGLIOSTRO, T. C. GOODALE

*Poulter Laboratory, Stanford Research Institute, Menlo Park, California 94025, U.S.A.*

### SUMMARY

One concern in the safety analysis of liquid metal fast breeder reactors (LMFBRs) is the release of radioactive core materials to the environment following a hypothetical core disruptive accident (HCDA). The release depends on the transport properties of the expanding, two-phase, fuel-coolant bubble produced during the HCDA and the energy available in the bubble to damage the reactor containment system. Most predictions of the HCDA bubble pressure-volume change relationship assume an isentropic expansion of the bubble material from some known initial state.

This work describes the development and characterization of an energy source that models the assumed initial conditions and the subsequent expansion of an HCDA bubble in a simple 1/30-scale model of the Clinch River Breeder Reactor (CRBR). The source is used in a study of the phenomena associated with expanding, rising HCDA bubbles, the transport of radioactive core materials to the cover gas region, and the loading resulting from the impact of the coolant slug with the vessel cover.

The source uses high-temperature, high-pressure water as the bubble material. The water, initially in the vessel's lower core, is released by opening an explosively driven, fast-opening valve between the lower and upper core barrel. When released, the water reaches a superheated state and flashes to vapor. The vapor expands out of the lower core, through the upper core barrel, and into the vessel containing the coolant simulant (water). High-speed photography is used to observe the expansion through the transparent walls of the vessel.

Characterization tests were performed with and without a vessel cover and with both nitrogen gas (1500 psi, room temperature) and water (1160 psi, 563 °F, 0% quality) as the bubble material. The surface motion, bubble volume, pressures in the lower and upper core, and the slug impact pressure were measured. From these, the displaced volume-time, entrainment-time, pressure-volume change, gaswork-volume change, and slug kinetic energy-volume change relations were derived.

The tests show the gaswork done by the bubble to be less (up to slug impact) than predicted by an isentropic expansion from the same initial conditions. The slug kinetic energy, in turn, is much less than the gaswork over the entire expansion. The low initial energy of the coolant slug and compression of the air in the cover gas volume cause the slug impact pressure to be one-fourth that predicted from the results of tests without a cover. A second slug impact occurs with an impact pressure one-half the magnitude of the first. Liquid entrainment in the bubble remains at 25% to 35% during most of the expansion.

We have developed and characterized a bubble source that simulates the qualitative behavior of flashing liquid-vapor fuel expansions during an HCDA. The results imply that gaswork and slug kinetic energy predictions based on an equilibrium expansion of a superheated liquid may be too high by a factor of two.

\* This work was supported by the Energy Research and Development Administration, Division of Reactor Development and Demonstration, Washington, D.C. 20545 under Contract No. E(04-3)-115.

## 1. Introduction

The liquid metal fast breeder reactor (LMFBR) accidents that are currently postulated to have the greatest potential for significant releases of radioactivity to the environment are those accidents involving core meltdown, called hypothetical core disruptive accidents (HCDAs). Safety technology research sponsored by ERDA is intended to assure that the risk to the public in the event of an HCDA is very low. A theoretical possibility exists that, during an HCDA, material motions and interactions might lead to rapid pressure-generation events that could cause significant structural damage to the reactor. In such an event, no significant releases of radioactivity could occur until radioactive materials were transported from the core to the leakage paths created in the reactor by the pressure excursion.

The objective of this experimental program is to provide basic information on the loads generated on the reactor cover and the phenomena of core material transport following an HCDA. The HCDA under study is a two-phase fuel ( $UO_2$ ) expansion that would result in a high-pressure core "bubble" that would expand out of the core and into the above-core sodium pool.

We have developed an energy source for modeling the expansion characteristics of the two-phase fuel bubble. The source will be used to develop an understanding of the dynamic and thermodynamic processes occurring in the bubble, the transport of radioactive core materials to the cover gas region, and the slug impact loads on the vessel cover, by simulating the HCDA in a simple, transparent, 1/30-scale model of the Clinch River Breeder Reactor (CRBR).

To simulate the bubble in our model, the bubble material is heated under high pressure in the lower core to a state that, when the pressure is suddenly released, causes the material to become superheated, to begin to flash to vapor, and to expand into the model through the upper core barrel as a two-phase bubble. Water is used as the bubble material and coolant simulant because its properties are well known and it is relatively safe at high temperatures.

Typical pressure-volume change ( $P-\Delta V$ ) curves are shown by the solid lines in Figure 1. The curves assume an isentropic expansion of the superheated  $UO_2$ . The curve characteristics of interest are their long flat shape and slow decay, unlike the expansion of sodium vapor shown as the broken line in Figure 1. The sodium vapor expansion has been simulated earlier by other energy sources that used either detonation products from low-density explosives or superheated steam [1]. As an aid in experiment design and in comparison of the experimental results with those of Figure 1, the expansion of the flashing water is assumed to be isentropic. This assumption can be valid only if:

- The heat transfer from the bubble is negligible during the period of interest (2 to 4 msec in our 1/30-scale model).
- The expansion is slow enough to allow the bubble material to remain in equilibrium; there must be time for vapor bubbles to grow in the superheated liquid and allow it to vaporize.

Figure 2 shows curves of pressure versus specific volume ( $P-v$ ) for the isentropic expansion of water from several initial states.

## 2. Source Development

A schematic of the flashing source apparatus is shown in Figure 3. The acrylic cylinder and upper core barrel form a simple 1/30-scale model of the interior of the Clinch River Breeder Reactor. This model does not include the upper core structure and the upper internal structure. The coolant simulant (water) fills the interior of the vessel to within 0.9 inch of the top cover.

The bubble material is held and heated in the lower core (Figure 4). Water completely fills the lower core and is heated by an Inconel heating element powered by a welding generator.

Before the experiment can begin, the heated, pressurized water in the lower core must be released into the upper core barrel by opening the passage between them. The passage must open completely in a time much shorter than the expansion time of the bubble in the vessel to ensure that the expansion of the bubble will not be affected by the way the passage is opened. An opening time one-tenth of the expansion time of the bubble in the vessel was considered adequate. Additionally, the pressure release mechanism must not interfere with the flow out of the lower core or release any debris into the vessel.

The mechanism chosen for development uses a pair of explosively driven sliding doors that seal the passage between the upper and lower core when closed. The doors are shown in place in Figure 3, and their opening sequence is shown in Figure 5. The doors are flat aluminum plates 0.285 inch thick and 3.2 inches wide that rest atop one another and slide in opposite directions. Each door is attached to a piston in a cylinder. The cylinders and the base for the acrylic vessel are held in alignment by large aluminum I-beams.

Figure 5(a) shows the piston-door assemblies in the closed position. Detonation of the low-density explosive\* drives the pistons outward. As the pistons move apart, the doors are pulled over one another and out of the passage. Once the passage is cleared, the piston-door assemblies are stopped by crushing aluminum honeycomb energy absorption material [Figure 5(c)]. The doors slide 3 inches before opening begins, allowing the doors to reach the high velocity necessary for adequate opening times with relatively low acceleration levels.

A 24-g explosive charge has produced opening times between 220 and 240  $\mu$ sec with the thick doors. These times are less than 1/10 the flashing bubble's measured expansion time of 2.5 msec. No "jetting" could be seen in the films as the doors opened, and the bubble was symmetric as it expanded, indicating adequately fast opening.

A fiducial was used to measure the motion of the entire vessel during the door opening sequence. Analysis of the film made of the test showed that total vessel motion was less than 1/16 inch and had no significant effect on the bubble behavior.

## 3. Characterization

Characterization tests have been performed on the flashing source with the vessel top cover both removed and in place. In both configurations water in the lower core was initially at 1160 psi, 563°F, and 0% quality. Only the test with the top cover in place will be described here. A complete report on the characterization experiments will be forthcoming.

---

\* A mixture of 90% PETN ( $C_5H_8O_{12}N_4$  pentaerythritol tetranitrate) and 10% plastic microspheres, by weight.

The experiment instrumentation is shown schematically in Figure 6. A high-speed camera films the bubble through the transparent acrylic vessel. Transducers mounted in the lower core ( $P_3$ ) and the upper core barrel ( $P_1$  and  $P_2$ ) record the pressure. Transducers in the top cover ( $P_4$ ,  $P_5$ , and  $P_6$ ) measure the slug impact pressure.

Figure 7 shows the movie sequence of the bubble expansion. In the first frame, the doors are just beginning to open. When the doors open, the water in the lower core begins to vaporize and expand, pushing water out of the core barrel and forming a water vortex at the core barrel opening (second frame), which grows (third frame) until the flashing water bubble emerges and engulfs it (fourth frame). The bubble expands, displacing the water slug until its impact with the top cover (eighth frame). The tenth frame, 580  $\mu$ sec after slug impact, shows the beginning of the first of three distinct periods of cavitation, each 480  $\mu$ sec apart, that follow slug impact. The cavitation sequence is seen in frames 11 through 15. Slug impact and cavitation will be discussed later.

The water surface motion is measured in each frame of the film to obtain a curve of water slug displacement versus time. This curve, with corrections for the compressibility of water and the elastic radial expansion of the vessel, is used to compute a curve of the displaced volume (the volume of the bubble material) versus time. The bubble silhouette is measured to compute a curve of the bubble volume (which includes the volume of the bubble material and the volume of the entrained liquid) versus time curve. The displaced volume versus time and bubble volume versus time curves are shown in Figure 8.

The pressure versus time (P-t) records of Figure 9 show that the lower core pressure drops sharply to approximately 700 psi, rises briefly to approximately 725 psi and then levels off at approximately 690 psi, and remains at that level until slug impact. The pressure drops sharply after the doors open because the resulting depressurization of the water in the core occurs before the water can begin to vaporize and expand rapidly. Once vaporization and expansion of the water begins, the pressure drop ceases as the expanding vapor fills the void left by the doors and begins to push against the water slug, accelerating it upward and causing the slight rise in pressure that follows the initial drop. As the slug acceleration decreases and the slug reaches a constant velocity, the pressure decreases slightly and maintains a constant value. At this point the water in the core is flashing and producing the vapor that pushes the water slug upward. The details of the processes involved in the expansion are being studied and will be reported on at a later date. The pressure increase seen in  $P_3$  after slug impact corresponds in time to the period during which the slug has moved away from the top cover as a result of the impact. Pressure in the upper core remains fairly constant after slug impact and during cavitation.

The pressure versus time records and the displaced volume versus time records are combined to yield curves of pressure versus volume change (P- $\Delta V$ ). The P- $\Delta V$  curves using the lower and upper core pressures are shown in Figure 10 along with the isentropic expansion of water from the same initial conditions. Since the experiment curve does not follow the isentropic curve, the expansion is not in equilibrium.

The P- $\Delta V$  curves are integrated to obtain the gas work done by the expanding bubble. The water slug displacement versus time curve is used to obtain the slug kinetic energy. These quantities are plotted against volume change in Figure 11. The slug kinetic energy curve peaks and falls off sharply in the last half of the expansion due to the slowdown of

the slug, which is attributed in part to compression of the air between the water surface and top cover. A pressure gradient exists in the bubble throughout the expansion, a result of the complex, two-phase nature of the expansion, nonequilibrium effects, condensation, and energy lost to turbulence at the vapor-liquid interface. The kinetic energy curve is the closest to the energy available to do damage.

Figure 12 shows the pressure versus time records of the transducers mounted in the top cover. The first spike is caused by slug impact, and its peak establishes the time of impact. Impact produces a pressure wave that moves down from the cover to the bubble; part of this wave is reflected back as an expansion wave. When this expansion wave reaches the cover, the slug rebounds from the cover, causing the pressure to fall to atmospheric, as seen on the records. The motion away from the top cover could compress the bubble and cause the momentary pressure increase or "hump" in the lower core pressure records mentioned above. A second impact occurs 3.3 msec later with a peak pressure 30% of the initial impact pressure.

The sharp spike from the first slug impact is due to the compression of the air between the water surface and the top cover. The displacement versus time record shows the final impact velocity to be 226 in./sec, which would result in an impact pressure, computed assuming a planar impact, of 1200 psi, which corresponds to the pressure 'plateau' seen on the back side of the first pulse of between 1000 and 1250 psi.

Cavitation, appearing as small bubbles, occurs after slug impact in all tests regardless of the source used. The bubbles are spherical and approximately the same size, 0.140 inch in diameter. In all tests, the cavitation is cyclic, appearing and disappearing two or more times. In test C-007 cavitation first occurs approximately 580  $\mu$ sec after slug impact and has a period of 180  $\mu$ sec ( $\pm 10\%$ ). The density of bubbles appears to be higher near the sides of the vessel, indicating that the bubbles are forming on the vessel walls, not throughout the water in the vessel.

Cavitation may result from interaction of expansion waves (caused by both the radial expansion of the vessel and the reflection of pressure waves from the free surface of the bubble and of the liquid in the vessel) originating from slug impact. The time of the first cavitation corresponds roughly to the time for a pressure wave to travel from the top cover to the vessel bottom and back to the top cover, where it is reflected as an expansion wave. The effect on the cavitation of the elastic expansion of the vessel and the deflection of the top cover is being studied and will be measured in future tests.

#### 4. Summary

The results of our preliminary work with 1/30-scale models can be summarized as follows:

1. The expansion is not in equilibrium and the experimental P- $\Delta V$  curves are lower than those for an isentropic expansion of water from the same initial conditions.
2. The measured slug kinetic energy is at most 27% of the slug kinetic energy from the P- $\Delta V$  curve of an isentropic expansion of water from the same initial conditions, and drops to 3.5% at slug impact.
3. The pressure gradient in the bubble implied by the difference in gas work and slug kinetic energy is due to nonequilibrium effects, condensation, turbulence of the entrained liquid, and error in the estimate of the slug mass.
4. The amount of entrained liquid remains at 25% to 35% of the total bubble volume throughout the expansion.

5. The bubble reaches a volume of 68.2 in.<sup>3</sup> at slug impact: the sum of the cover gas volume (47.5 in.<sup>3</sup>) and the volume of entrained liquid (20.7 in.<sup>3</sup>). At slug impact, the top of the bubble is 4.0 in. above the core and 5.2 in. in diameter.

6. The water slug impact pressures are low because of the low energy of the coolant slug at impact, the energy lost in compressing the cover gas, and the resulting increased condensation of vapor in the bubble.

7. The water slug rebounds from the vessel cover after the first impact and impacts it a second time 3.3 msec after the first with a peak pressure approximately one-half that of the first impact.

8. A cyclic cavitation of the coolant was observed after slug impact. Cavitation first occurs approximately 580  $\mu$ sec after slug impact and has a period of 480  $\mu$ sec ( $\pm 10\%$ ).

9. The bubble breaks up into segments as it leaves the core barrel at times after slug impact.

Before additional experiments are performed, we will study the postulated LMFBR fuel-vapor expansion in more detail and, through relevant scaling laws, relate prototypic phenomena to phenomena observed in our scale model experiments. One important phenomenon observed in our experiments is the nonequilibrium expansion of the flashing water bubble, which lowers the energy in the bubble available to do damage.

Once the relation between prototypic and observed scale model phenomena is better understood, we will continue characterization tests at different initial conditions to determine how bubble behavior is affected by the initial condition parameters (pressure, temperature, quality, and total mass). The bubble's internal structure will be studied with x rays of the bubble expanding in a two-dimensional model of the reactor vessel. The source will then be used to study the transport of radioactive materials from the core to the cover gas region.

To improve the apparatus and CRBR model, we will develop the fast-opening valve further and add more details, such as the upper core structures and upper internal structures of the reactor.

#### References

- [1] CAGLIOSTRO, D. J., "High Pressure Vapor Expansion Experiments," Safety Technology Meeting on Radiological Consequence Assessment, Canoga Park, California (July 30-31, 1975).

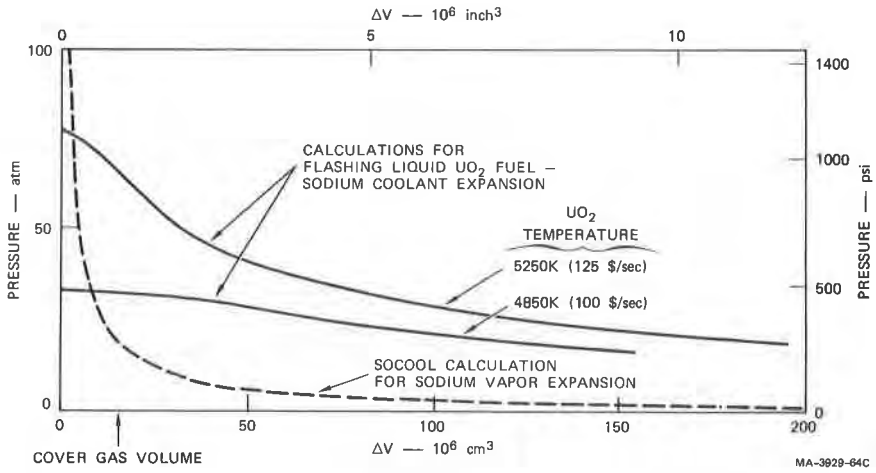


FIGURE 1 PREDICTED PRESSURE-VOLUME CHANGE CURVES FOR THE HCDA BUBBLE

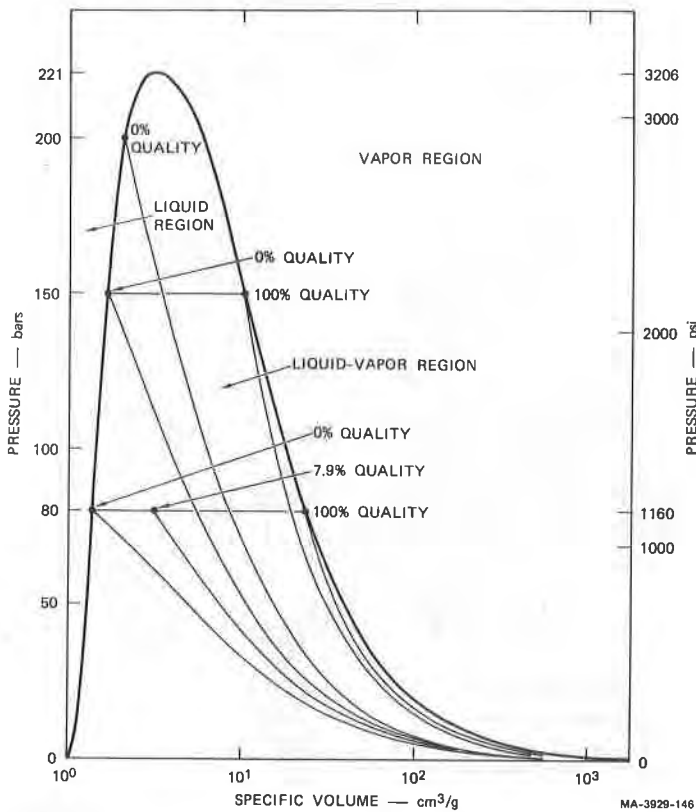


FIGURE 2 ISENTROPIC EXPANSION OF WATER FROM SEVERAL INITIAL STATES

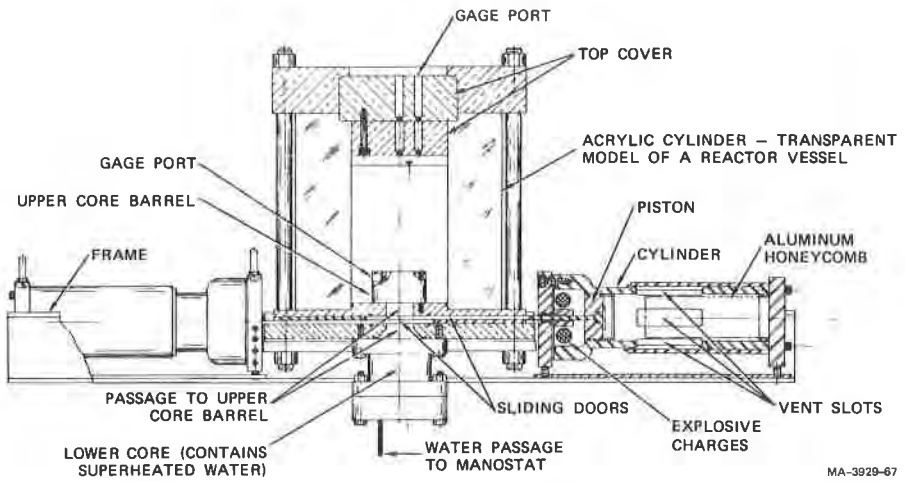


FIGURE 3 COMPLETE FLASHING SOURCE ASSEMBLY

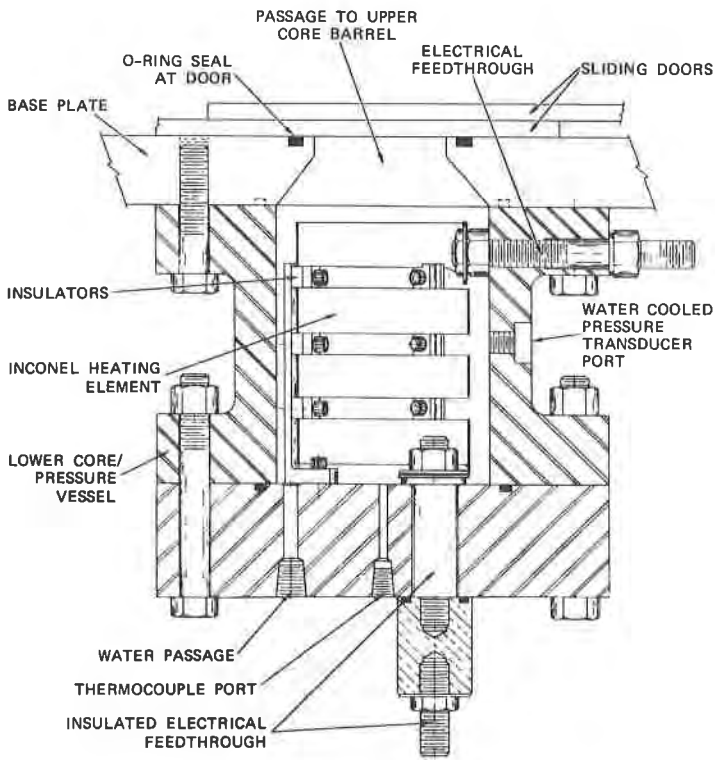


FIGURE 4 LOWER CORE HEATING ELEMENT DETAIL



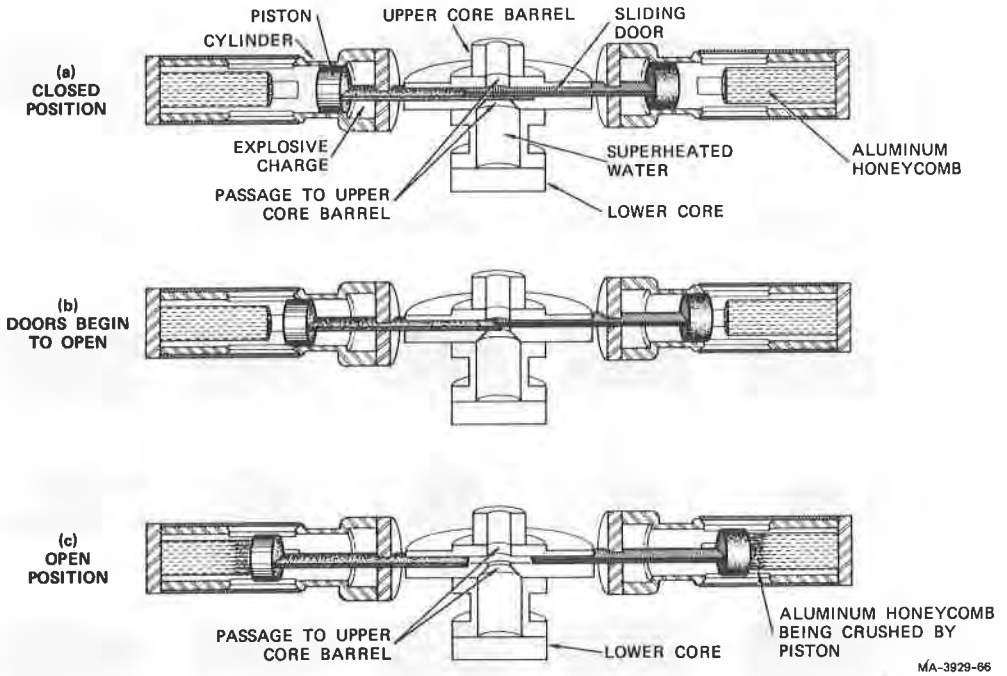


FIGURE 5 SLIDING DOOR OPENING SEQUENCE

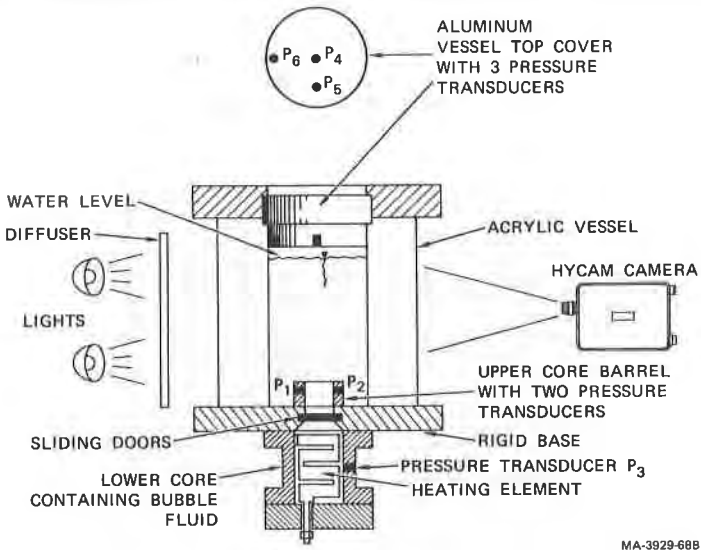


FIGURE 6 INSTRUMENTATION SCHEMATIC

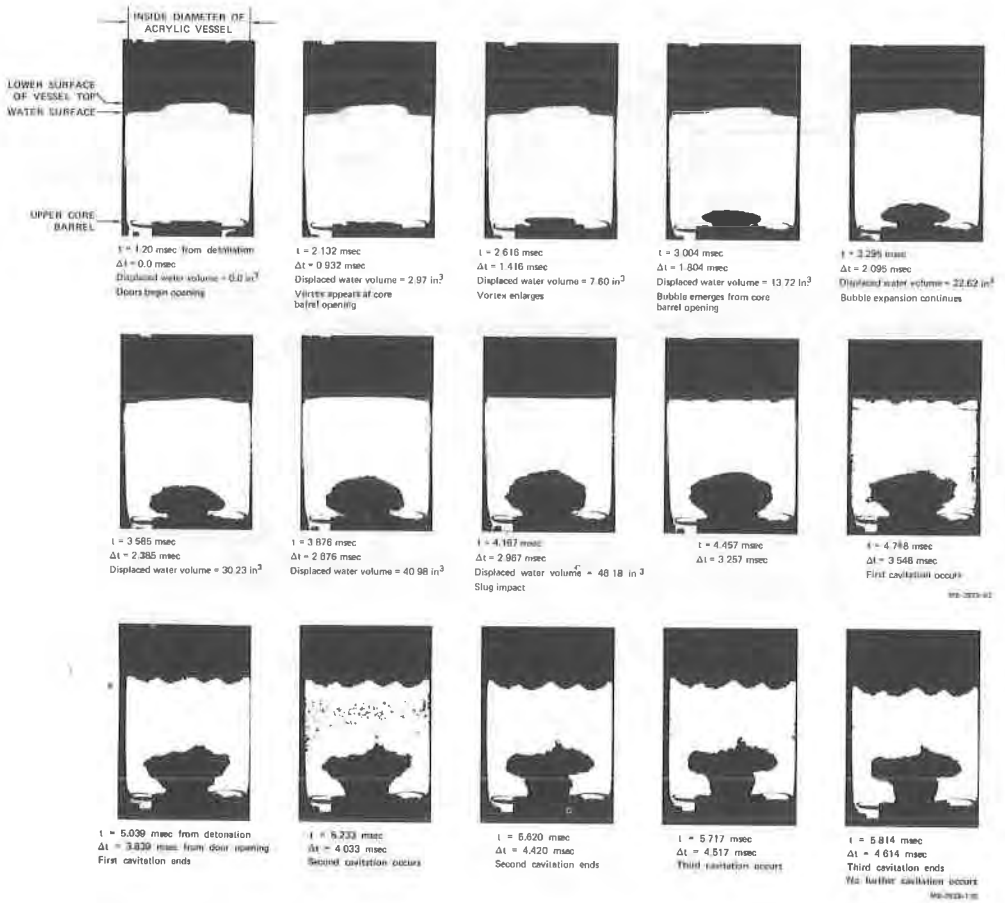


FIGURE 7 BUBBLE EXPANSION PHOTO SEQUENCE

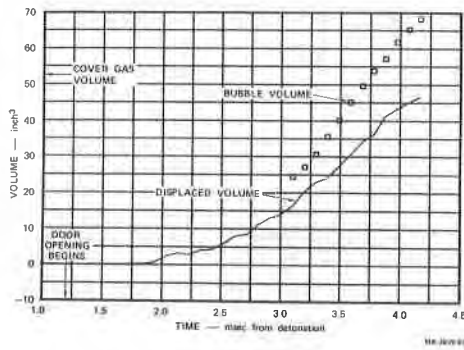


FIGURE 8 BUBBLE VOLUME/DISPLACED WATER VOLUME VERSUS TIME

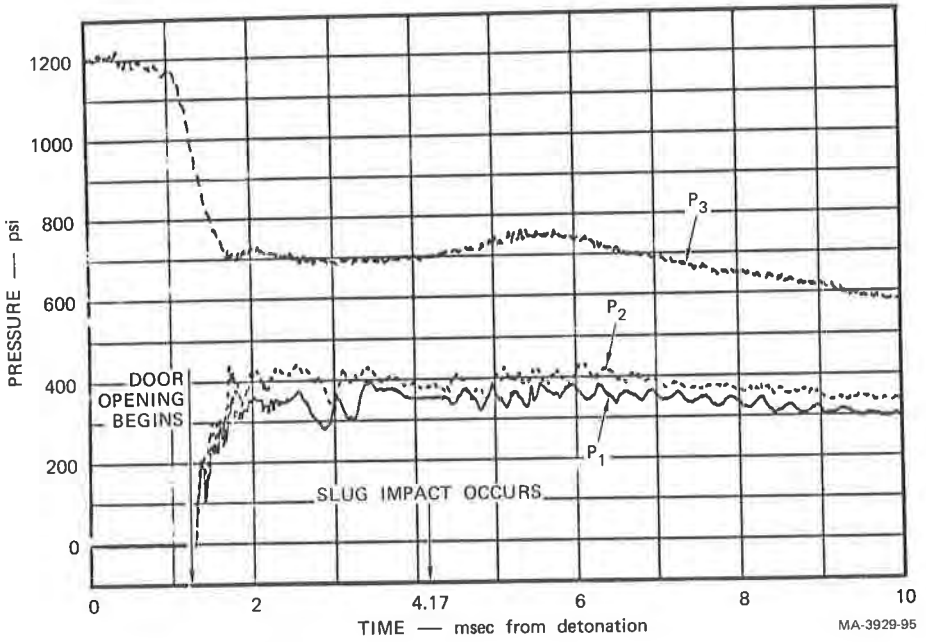


FIGURE 9 LOWER CORE (P<sub>3</sub>)/UPPER CORE (P<sub>1</sub>, P<sub>2</sub>) PRESSURES VERSUS TIME

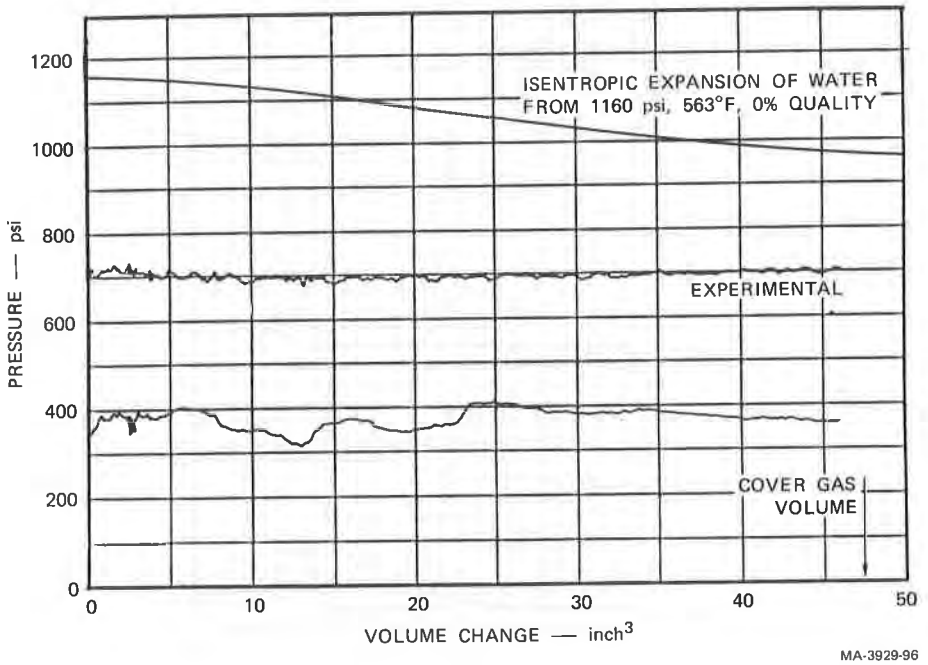


FIGURE 10 LOWER CORE AND AVERAGE UPPER CORE PRESSURE VERSUS VOLUME CHANGE EXPERIMENTAL AND PREDICTED RESULTS

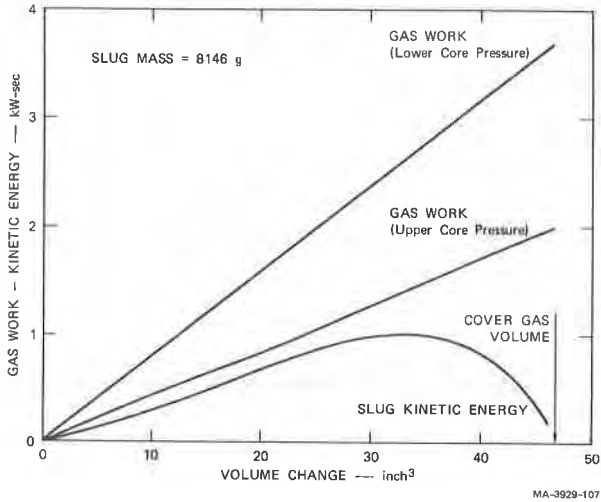


FIGURE 11 GAS WORK AND SLUG KINETIC ENERGY VERSUS VOLUME CHANGE

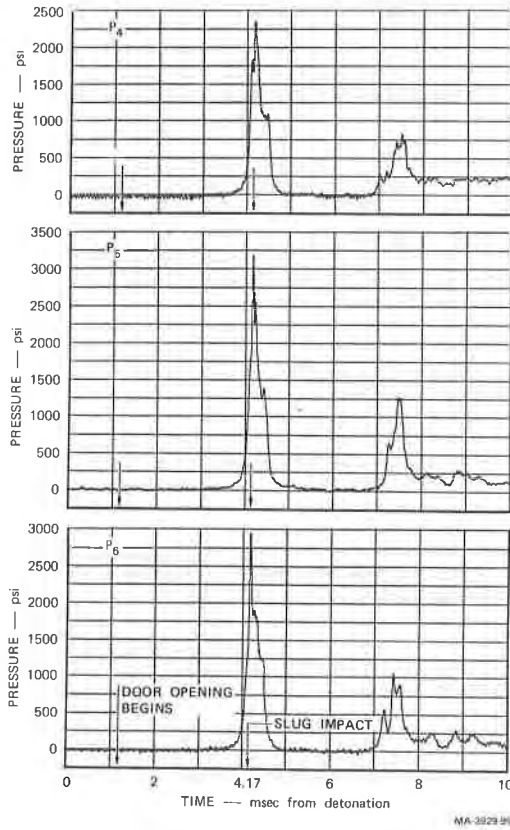


FIGURE 12 VESSEL TOP COVER PRESSURE VERSUS TIME